The real-time atmospheric turbulence modeling and compensation with use of adaptive optics

Anna Lylova[a], Alexis Kudryashov[a,b], Julia Sheldakova[b], Gilles Borsoni[c]

[a]University of Mechanical Engineering, Adaptive Optics Laboratory,
Bolshaya Semenovskaya str., 38, Moscow, 107023
[b]V.E. Zuev Institute of Atmospheric Optics SB RAS (IAO SB RAS),
Academician Zuev square, 1, Tomsk, Russia, 634021
[c]AKA Optics SAS, Hotel Technoptic,
2 rue Marc Donadille, Marseille, France, 13013

ABSTRACT

It is suggested to reconstruct the phase screens with the use of stacked-actuator deformable mirror and to compensate for the introduced distortions by the bimorph mirror. The reproducing and correction results are presented in the paper. The problems of the reconstruction and compensation are discussed.

Keywords: atmospheric turbulence, adaptive optics, bimorph deformable mirror, stacked-actuator deformable mirror, Shack-Hartmann wavefront sensor

1. INTRODUCTION

Atmospheric turbulence refractive index fluctuations lead to the distortions of the light waves propagated through the atmosphere. This phenomenon limits the telescopes resolution and disturbs the laser irradiance coherence that worsen the image quality and reduce the laser power. The problem of the wavefront distortions compensation could be solved by means of adaptive optics. The correction technique is rather well-developed but the experiments might be hard-implemented and very expensive. Thus, we suggested to design the real-time high-precision model of the atmospheric turbulence and try to correct for these distortions in the lab.

To reproduce and compensate for the phase distortions we used two different types of deformable mirrors: stacked-actuator one to model the turbulence distortions and bimorph one to corrector for them.

2. SETUP

Our work was divided into two steps:
1) Modeling of the atmospheric turbulence in lab by stacked-actuator deformable mirror[1]:
    - Phase screen modeling with applying the FFT to the Kolmogorov spectrum of the phase fluctuations[2,3].
    - Calculation of the control voltages to apply them to the actuators of the mirror,
    - Reconstruction of the modeled phase screen with the deformable mirror.
2) Correction of the reconstructed phase screen with bimorph deformable mirror[4,5]:
    - Analysing of the phase screen with Shack-Hartmann wavefront sensor[6],
    - Calculation of the control voltages to apply them to the electrodes of the bimorph deformable mirror.
    - Compensation for the phase fluctuation.

Experimental setup is presented on fig. 1. The collimated beam went to the stacked-actuators deformable mirror, then was reflected to the bimorph deformable mirror, passed through the telescope, and was analysed by Shack-Hartmann wavefront sensor. The voltages applied to the stacked-actuators mirror by Control Unit 1 were calculated by PC1 according to the analytical model to reproduce turbulence with some predefined parameters. To control for the bimorph mirror the voltages to be set by Control Unit 2 were calculated by PC 2 based on the information from Shack-Hartmann wavefront sensor to compensate for the measured aberrations introduced by the stacked-actuators mirror.

Traditional Shack-Hartmann wavefront sensor consists of a two-dimension microlenses array (lenslet) and CCD or CMOS camera. Lenslet divides a wavefront of the incoming beam into a number of cells and forms an ensemble of the focal spots that should be registered by camera. It is considered that in the region of a single cell the only aberration of

the wavefront is tilt. The displacement of each focal spot from the ideal, reference, position is proportional to the wavefront local slope value. Therefore, by measuring the local slopes of the incoming beam we are able to reconstruct the wavefront[8,9]. Shack-Hartmann wavefront sensor parameters are presented in table 1.
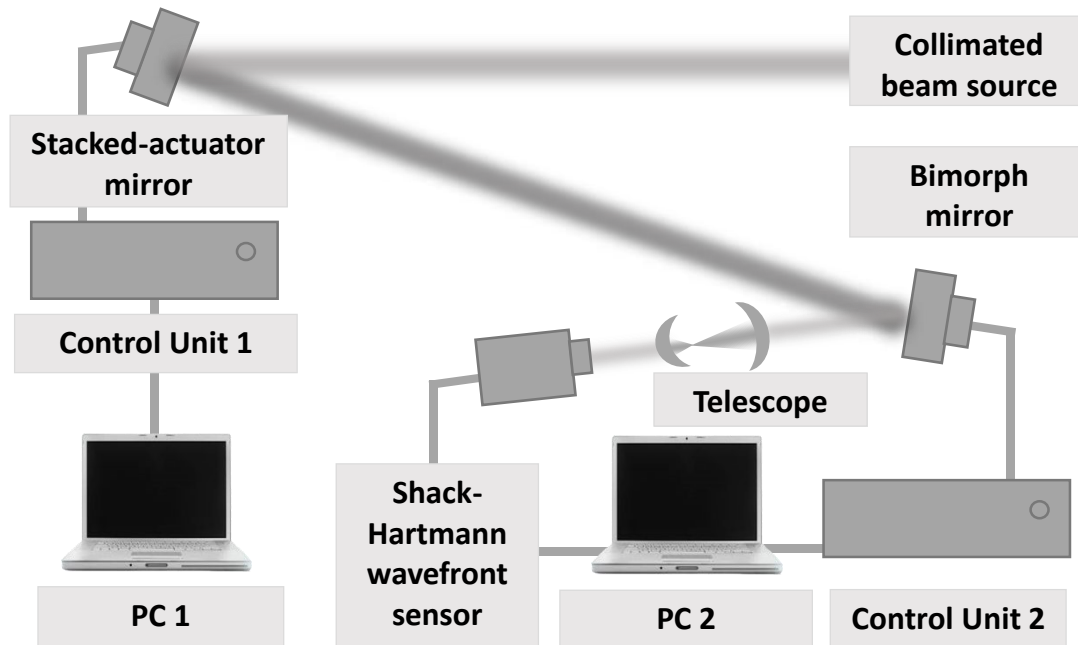

Fig. 1. Scheme of the adaptive optical system.

Table 1. Parameters of Shack-Hartmann wavefront sensor.

Parameter	Value
Spectral bandwidth	350 – 1100 nm
Data acquisition	Up to 25 Hz
Computer Interface	USB 2.0
Lenslet pitch	160 μ
Lenslet array focal length	5 mm

3. ALGORITHM OF THE PHASE SCREEN MODELING

To provide an experiment we generated a sequence of the phase screens and tried to compensate them with the use of the adaptive optical system. To reproduce the phase screens we applied the Fast Fourier transform to the Kolmogorov spectrum of the phase fluctuations[10].

$$p(u,v,t+\Delta t) = \int\limits_{-\infty}^{\infty}\int\limits_{-\infty}^{\infty} \sqrt{K(x,y)} \cdot f(x,y,t+\Delta t) \cdot \exp(i \cdot \sqrt{x^2 + y^2} \cdot V \cdot \Delta t)dxdy, \qquad (1)$$

where $p(u,v,t+\Delta t)$ – phase screen at the time moment $t+\Delta t$, (x,y) – point of the spectrum, (u,v) – point of the phase screen, V – wind velocity, t - time of the previous phase screen, $t+\Delta t$ - time of the new phase screen, Δt – time between two phase screens, $K(x,y)$ – the spectrum of the phase fluctuations

$$K(x,y) = 0.023 \cdot (\frac{2D}{r_0})^{\frac{5}{3}} \cdot (x^2 + y^2)^{\frac{11}{3}}, \qquad (2)$$

where D - aperture diameter, r_0 - Fried parameter, $f(x,y,t+\Delta t)$ is defined as

$$f(x, y, t + \Delta t) = p \cdot f(x, y, t) + \sqrt{1 - p^2} \cdot \exp(i \cdot \varphi(x, y, t)), \tag{3}$$

where $p = \exp(\dfrac{-\Delta t}{\tau})$, τ – atmosphere coherence (freezing) time, $\varphi(x, y, t)$ – random delta-correlated value in the range of $[0, 2\pi]$

$$f(x, y, t = 0) = \exp(i \cdot \varphi(x, y, t = 0)), \tag{4}$$

To normalize the phase values in correspondence with the $\dfrac{D}{r_0}$ value the phase structure function was used:

$$D = 6.88 \cdot (\frac{\sqrt{x^2 + y^2}}{r_0})^{\frac{5}{3}}, \tag{5}$$

Then, each calculated phase screen was represented as an ensemble of response functions and reconstructed by deformable mirror.

4. DEFORMABLE MIRRORS

STACKED-ACTUATOR DEFORMABLE MIRROR

A stacked-actuator deformable mirror perfectly reproduces atmospheric phase fluctuations because of the high spatial resolution. This type of wavefront correctors consist of an array of stacked actuators glued to the substrate. Scheme of the actuators and design of the mirror is presented by fig. 2. Application of voltages to the stacked actuator produces extension (or reduction, depending on the sign of the voltages vs polarization) of the actuator and this results in the deformation of the reflective surface. In our experiment, we used a mirror with just 19 actuators. The voltage values varied from -30V to +130 V. The interferograms of some response functions are presented on fig. 2. The main parameters of the wavefront corrector are given in table 2.
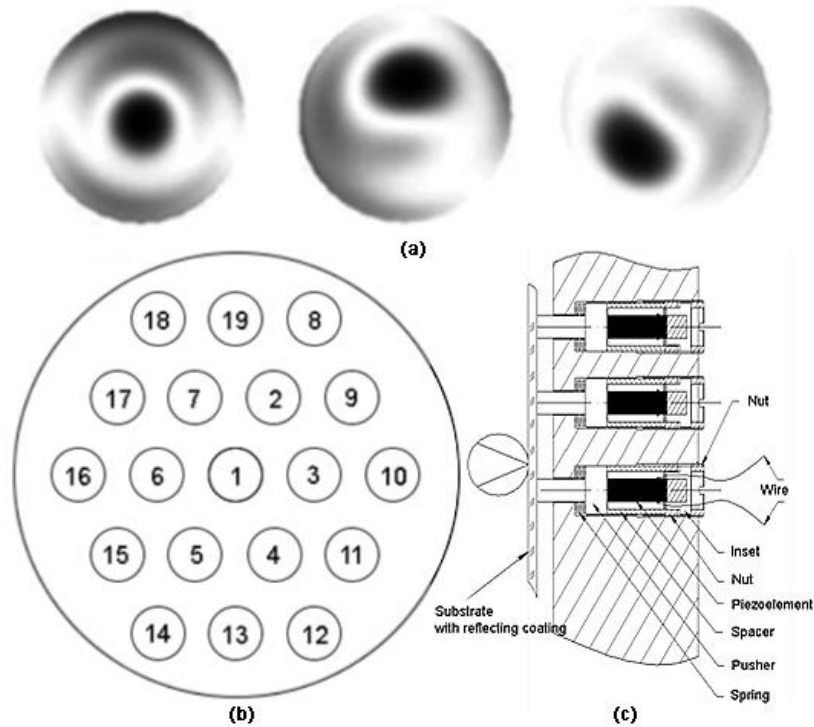

Fig 2. (a) Interferograms of some response functions, (b) scheme of the actuators,
(c) scheme of stacked-actuator deformable mirror.

Table 2. Characteristics of the bimorph deformable mirror.

Mirror type	stacked-actuator
Mirror diameter	40 mm
Active diameter	35 mm
Mirror substrate	glass
Actuator type	PZT
Frequency bandwidth	2 KHz
Control actuators number	19
Control voltage range	-30…+130V

According to our calculations, the contribution of the higher-order aberrations is rather small and the desired phase screens could be reconstructed by 15 Zernike polynomials. Thus, according to our suggestion a 19 channel mirror should be enough.

BIMORPH DEFORMABLE MIRROR

Main advantage of the bimorph mirrors is the ability of low-order aberrations reproduction. Fig. 3 presents the design, scheme of the electrodes, and some response function interferograms of the bimorph mirror we used for our work. Traditional bimorph mirror consists of a comparatively thick glass substrate firmly glued to thin actuator piezoelectric ceramic disks (Fig. 3 a). The electrical signal applied to the electrodes causes piezo-disk expanding or shrinking (depending on the polarization and the sign of the applying voltage). Thus, glued substrate is trying to prevent expansion and, as a result, the mirror surface bends. To reproduce different types of aberrations using bimorph deformable mirror the outer electrode is divided in several control electrodes as it is shown on fig. 3 b. Applying the voltage to the electrode causes the local bending of the mirror shape. The rest mirror surface deforms according to the boundary conditions. This type of deformation is due to the modal wavefront correctors. The size and the electrodes number of the mirror is defined according to the aberration that have to be reproduced or corrected. The main parameters of the wavefront corrector are given in table 3.
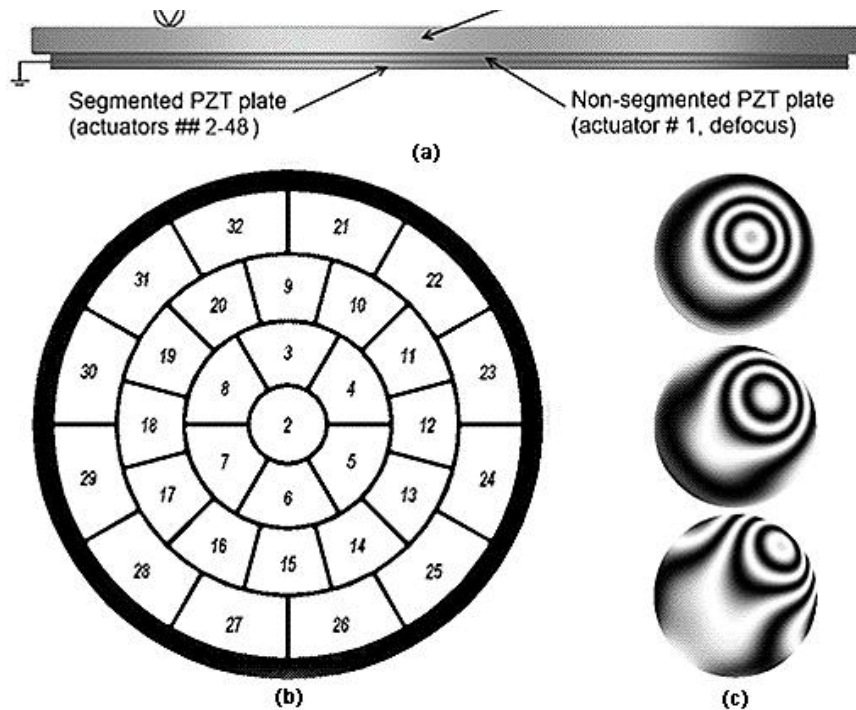

Fig 3. (a) Scheme of bimorph deformable mirror, (b) scheme of the electrodes,
(c) interferograms of the response functions.

Table 3. Characteristics of the bimorph deformable mirror.

Mirror type	bimorph
Mirror diameter	35 mm
Active diameter	30 mm
Mirror substrate	glass
Actuator type	PZT disc
Frequency bandwidth	7 KHz
Control electrode number	32
Control voltage range	-200…+300 V

5. EXPERIMENTAL RESULTS

Table 4 presents the result of phase screen reconstruction by stacked-actuator deformable mirror. The approximation of the modeled phase screen according to Kolmogorov statistics ($D/r_0 = 10$), the phase screen reconstructed by stacked-actuator mirror, and the difference between them are presented in table 4.

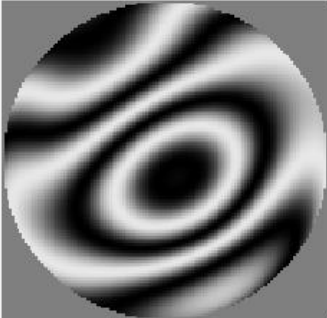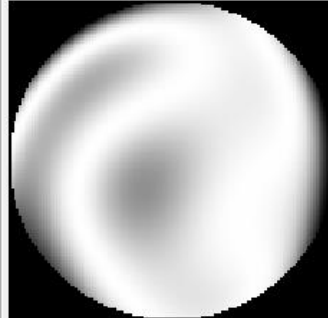Table 4. Interferograms, PV and RMS of the reconstructed phase screens.

	Modeled phase screen	Reconstructed phase screen	Difference phase screen
Inreferograms			
PV, μ	1.113	0.958	0.348
RMS, μ	0.227	0.200	0.050

Table 4 demonstrates that the stacked-actuator mirror provides rather good reconstruction. But it should be noticed that the modeled phase screens and the reconstructed ones differ from each other. This phenomena is caused by hysteresis effect of piezoceramics. It means that the extension or shrinking of the actuators depends not only on the applied voltages, but also their history[11]. Fig. 4 demonstrates the influence of the hysteresis effect on the amplitude of the mirror deformation. At every iteration response has some delay caused by the previous values of the input and output signals. To correct for the hysteresis effect of piezoceramics one needs at least three iterations.
Also for better phase screen reproducing a mirror with higher spatial resolution could be used.
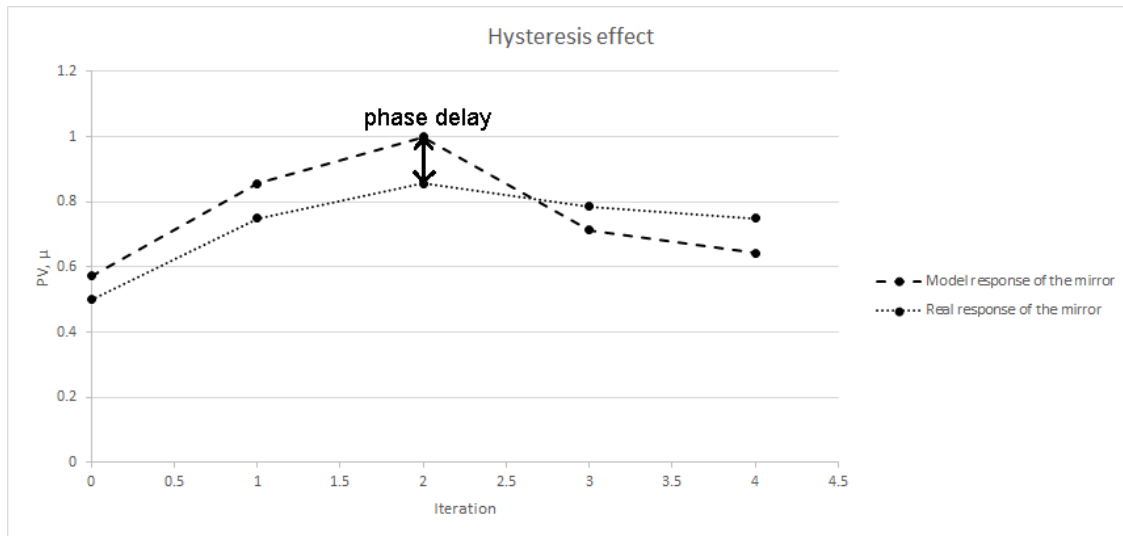
Fig. 4. Hysteresis effect influence on the response of the mirror.

Fig. 5 presents the result of the phase screen compensation by bimorph deformable mirror. Zernike polynomials absolute values varied from 0.001 μ to 0.012 μ. P-V was 0.098 μ, RMS was 0.015 μ. Thus, the bimorph deformable mirror provides rather good compensation of the phase screen that was simulated by stacked-actuator deformable mirror.
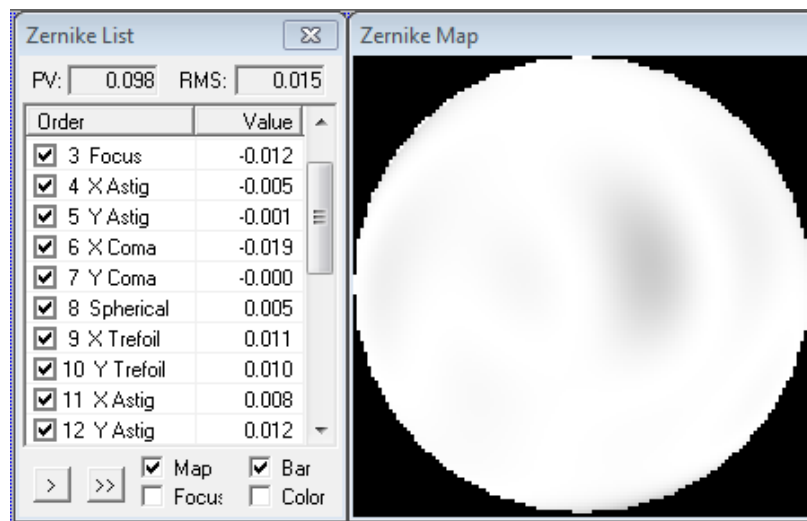

Fig. 5. The phase screen compensation results: Zernike polynomials values and interferogram.

6. CONCLUSION

In our work, we found out that the stacked-actuator deformable mirror provides a good phase screen reconstruction. We reproduced the phase screens with the designed adaptive system. We investigated the reconstruction problems and proposed methods for the solution of these problems. Also we compensated for the phase distortions by means of bimorph deformable mirror and investigated that this type of the wavefront corrector provides a good compensation of the phase distortions that were reproduced by the stacked-actuator deformable mirror.
For the future research, we plan to design the stacked-actuator deformable mirror with higher spatial resolution and to compare the reconstruction results.

ACKNOWLEDGMENTS

REFERENCES

[1]   M. Laslandes, K. Patterson, S. Pellegrino, "Optimized actuators for ultrathin deformable primary mirrors", Applied Optics **54**(15), 1559 (2015).

[2]   R. G. Lane, A. Glindemann and J. C. Dainty "Simulation of Kolmogorov phase screen", Waves in Random Media 2, 209-224 (1992).

[3]   L. Burger, I. A. Litvin, and A. Forbes, "Simulating atmospheric turbulence using a phase-only spatial light modulator," South African Journal of Science 104, 129-137 (2008).

[4]   V. Samarkin, A. Aleksandrov, and A. Kudryashov, "Bimorph mirrors for powerful laser beam correction and formation," J. D. Gonglewski, M. A. Vorontsov, M. T. Gruneisen, Ed., Proc. SPIE **4493**, 269-276 (2002).

[5]   A. V. Kudryashov and V. I. Shmalhausen, "Semipassive bimorph flexible mirror for atmospheric adaptive optics applications," Optical Engineering **35**(11), 3064-3073 (1996).

[6]   A. Kudryashov, V. Samarkin, and A. Aleksandrov, "Adaptive optical elements for laser beam control," U. Efron, Ed., Proc. SPIE **4457**, 170-178 (2001).

[7]   A. Rukosuev, A. Alexandrov, V. Zavalova, V. Samarkin, and A. Kudryashov, "Adaptive optical system based on bimorph mirror and Shack-Hartmann wavefront sensor," J. D. Gonglewski, M. A. Vorontsov, M. T. Gruneisen, Ed., Proc. SPIE **4493**, 261-268 (2002).

[8]   R. G. Lane and M. Tallon, "Wave-front reconstruction using a Shack–Hartmann sensor," Applied Optics **31**(32), 6902-6908 (1992).

[9]   D. R. Neal, J. Copland, D. Neal, "Shack-Hartmann wavefront sensor precision and accuracy," Proc. SPIE **4779**, 148-160 (2002).

[10] V. Dudorov, V. Kolosov, G. Filimonov, "Algorithm for formation of an infinite random turbulent screen", Proc. SPIE **6160**, 61600R1-61600R8 (2006).

[11] S. Cornelissen, A. Hartzell, J. Stewart, T. Bifano, P. Bierden, "MEMS Deformable Mirrors for Astronomical Adaptive Optics", edited by Brent L. Ellerbroek, Michael Hart, Norbert Hubin, Peter L. Wizinowich ed. Adaptive Optics Systems II, Proc. SPIE **7736**, 77362D (2010).